ARTICLE

Electrostatically modulated magnetophoretic transport of functionalised iron-oxide nanoparticles through hydrated networks

Received 00th January 20xx,
Accepted 00th January 20xx

DOI: 10.1039/x0xx00000x

Stephen Lyons,[a] Eoin P. Mc Kiernan,[b] Garret Dee,[c] Dermot F. Brougham,[b*] and Aoife Morrin [a*]

Factors that determine magnetophoretic transport of magnetic nanoparticles (MNPs) through hydrated polymer networks under the influence of an external magnetic field gradient were studied. Functionalised iron oxide cores (8.9 nm core diameter) were tracked in real-time as they moved through agarose gels under the influence of an inhomogeneous magnetic field. Terminal magnetophoretic velocities were observed in all cases, these were quantified and found to be highly reproducible and sensitive to the conditions. Increasing agarose content reduced magnetophoretic velocity, we attribute this to increasingly tortuous paths through the porous hydrated polymer network and propose a new factor to quantify the tortuosity. The impact of MNP surface functionalisation, charge, network fixed charge content, and ionic strength of the aqueous phase on velocity were studied to separate these effects. For MNPs functionalised with polyethylene glycol (PEG) increasing chain length reduced velocity but the tortuosity extracted, which is a function of the network, was unchanged; validating the approach. For charged citrate- and arginine-functionalised MNPs, magnetophoretic velocities were found to increase for particles with positive and decrease for particles with negative zeta potential. In both cases these effects could be moderated by reducing the number of agarose anionic residues and/or increasing the ionic strength of the aqueous phase; conditions under which tortuosity again becomes the critical factor. A model for MNP transport identifying the contributions from the tortuous pore network and from electrostatic effects associated with the pore constrictions is proposed.

Introduction

Detailed understanding of the transport of nanoparticles (NPs), and in particular magnetic nanoparticles (MNPs), through biological matrices such as the extracellular matrix (ECM) or other collagenous materials[1,2] will be key in enabling the development of responsive transdermal drug and gene delivery systems, target capture methods[3,4] and hyperthermic cancer treatment.[5] However, a necessary first step is to study the response of MNPs to applied magnetic fields in bio-mimetic environments, work which will pave the way for developing *in vitro* and *in vivo* applications.[2] The diffusive movement of particles in tissue depends on size, charge, and surface chemistry as well as the physicochemical properties of the tissue matrix.[6] In the case of the complex suprastructure of the ECM, particles undergo Brownian motion through the pores within the network. Particle transport is influenced by both the physical and chemical nature of the network in distinct ways; (i) direct electrostatic interactions with matrix fibres for charged particles, (ii) direct steric interactions, and (iii) indirect hydrodynamic interactions, *i.e.* on approaching fibres the restricted motion of water molecules slows particle diffusion. A similar picture is anticipated for particle motion though the pore network of other polymer structures including hydrogels. Hydrogels can serve as basic physical models of tissue,[7–9] for studying nanoparticle transport.[2]

[a] *Insight SFI Research Centre For Data Analytics; National Centre for Sensor Research; School of Chemical Sciences, Dublin City University, Ireland.*
[b] *School of Chemistry, University College Dublin, Ireland.*
[c] *School of Chemistry, Trinity College Dublin, Ireland*
† Footnotes relating to the title and/or authors should appear here.
Electronic Supplementary Information (ESI) available: [details of any supplementary information available should be included here]. See DOI: 10.1039/x0xx00000x

Directional transport of NPs may be controlled by fluid flow, chemical gradients or by applying light, electric or magnetic fields.[10] In the case of iron oxide MNPs, inhomogeneous magnetic fields exert a force on the particle proportional to its magnetic volume, to the field strength, and to the gradient of the field.[11] MNPs migrate up the field gradient region, with the opposing viscous force governed by the viscosity of the matrix and scaling with the particle (average) hydrodynamic diameter (d_{hyd}). Significant magnetic forces are required to manipulate movement of MNPs.[12] Neodymium alloys or electromagnets are known to induce sufficient forces over tens of millimetres[13]. Hence, as magnetic fields permeate cells and tissue, magnetophoretic motion can be used to guide MNPs through biological tissue.

An early study by Holligan *et al.* reported magnetophoretic motion of 10 nm iron oxide MNPs in agarose gels (a model for vitreous humour) using spatially directed magnetic forces.[14] By equating the magnetic and drag forces theoretical terminal velocities were calculated to support the experimental findings. A similar study based on measuring and predicting the terminal velocity of MNPs through purified ECM matrix was carried out by Kuhn *et al.*[15] Very recently, magnetophoretic transport was studied for drug delivery to solid tumours[2]. Magnetophoretic velocity measurements were taken in this case in a similar manner as previous works and MNP transport was studied in both agarose and excised tissue. It was demonstrated that tissue penetration increased 5-fold using oppositely polarised external magnets, as opposed to a single magnet, with the additional benefit that a constant field gradient could be applied in both axial and radial directions using the configuration described.

For *in vivo* and *in vitro* applications superparamagnetic particles are favoured; their small size is likely to minimise tissue damage and the absence of bulk magnetisation at zero field improves colloidal stability and hence shelf life.[16] Magnetophoretic motion of MNPs through gels or tissue will be affected by local interactions with polymer chains of a hydrogel or collagen protein of the ECM, respectively. These interactions will include electrostatic, steric and hydrodynamic contributions. Specifically, the influence of electrostatic interactions between the surrounding network and the MNPs during magnetophoresis has not been described for either synthetic hydrogels or ECM. Given the complexity and highly ionic nature of the ECM tissue environment (collagen type I the most abundant fibrillar protein in connective tissue ECM has ~15–20% ionisable peptide residues)[17] assessment of the electrostatic impact on magnetophoretic motion in simpler charged porous media is required for development of more advanced matrices for magnetophoretic applications.

Here, the motion of functionalised MNPs through an agarose gel medium, under the influence of an inhomogeneous magnetic field is studied. MNP motion was tracked optically in gel media by observing migration of the MNP front over time. All MNP suspensions exhibited linear displacements with time, confirming the attainment of a terminal magnetophoretic velocity under the conditions tested. The observed velocities were not consistent with the predictions of a simple model for the viscosities experienced by the MNPs during transport. A single factor is introduced which successfully accounts for the tortuous path that MNPs experience during magnetophoresis. It was found that in the absence of electrostatic interactions, or when these are substantially reduced, a single tortuosity is observed for a given agarose content. Critically MNP surface charge was found to modulate magnetophoretic velocity, with positively charged MNPs travelling faster and negatively charged MNPs slower than anticipated. A model for particle transport through networks comprised of hydrophilic chains is proposed wherein interactions at the pore constrictions (entrances and exits) determine the electrostatic contribution to magnetophoretic velocity. The implications of electrostatic modulation for magnetophoretic-driven movement of particles in porous polymeric networks such as tissue are discussed.

Experimental

Reagents and equipment

Iron acetylacetonate (14024-18-1), benzyl alcohol (100-51-6), (3-Glycidyloxypropyl)trimethoxysilane (GLYMO) (2530-83-8), end terminal aminated polyethylene glycol (PEG) MW400, MW1000, MW2070 (25322-68-3), acetone (67-64-1), sodium citrate tribasic(III) (6132-04-3), chloroform (67-66-3), tetrahydrofuran (THF) (109-99-9), potassium hydroxide (1310-58-3), hydrochloric acid (7647-01-0), agarose (9012-36-6) (low electroendosmosis (EEO)) (0.09-0.13), agarose (medium EEO) (0.16-0.19), agarose (high EEO) (0.23-0.26), aqueous ammonia (1336-21-6) and phosphate buffered saline (PBS) tablets (78392) were all purchased from Sigma. L-arginine (74-79-3) was purchased from Biochemika. A 50 x 25 mm grade N52 neodymium magnet (F335-N52) was used for all magnetophoresis studies and was purchased from www.first4magnets.com.

Materials synthesis and methodology

MNP synthesis: MNPs were synthesised using an adaptation of the Pinna method[18]. Briefly, the MNPs were formed by mixing iron acetylacetonate (1 g) with benzyl alcohol (20.0 mL). This mixture was placed into a G30 glass test tube and microwave digested for 3 h at 200°C under pressure (18 bar). The resulting dispersion was 50.0 mg/mL of Fe_2O_3 MNPs and the core diameter was determined to be 8.9 ± 0.8 nm by Transmission Electron Microscopy (TEM) carried out using a FEI Tecnai G2 20 TWIN 200kV (Fig S1) whereby 5 µL of suspension was pipetted onto a carbon TEM grid and allowed to air dry overnight before imaging.

Magnetometry: The Vibrating Sample Magnetometer (VSM) measurements on the synthesised cores were performed on a homemade VSM assembled by the Coey Magnetics Group. The VSM can scan across an applied field from -1.1 to 1.1 T at room temperature. The VSM was calibrated before running samples with a pure Nickel sample of known mass. Nickel is a ferromagnetic material with a known magnetic moment of 55.4 $A{\cdot}m^2/kg$ at 1 T at room temperature. After calibration, a sample was loaded into a non-magnetic plastic holder, sealed with a cap and loaded into the VSM. This sample was then scanned across the magnetic range of the VSM to give the characteristic hysteresis loop of that sample to determine magnetisation saturation (Fig S2).

MNP functionalisation: To functionalise the MNP surface with PEG or arginine, GLYMO-functionalised MNPs were first synthesised according to Brougham et al.[19] Briefly, 2.0 mL of MNPs (1.0 mg/mL) was added to a vial with 4 mL of acetone. This caused the MNPs to precipitate out of the benzyl alcohol. The glass vial was then placed on a magnet to retain the MNPs while the benzyl alcohol/acetone mixture was removed. This step was repeated 3 times to ensure all benzyl alcohol was removed. GLYMO (50.0 µL) was dissolved with chloroform (2 mL) and added to the MNP material. This mixture was then placed on a plate shaker at 400 rpm for 24 h. THF (2 mL) was

used to remove excess GLYMO by magnetic separation after agitation.[19]

To prepare PEG-MNPs[19], PEG (7.0 µL) was dissolved in THF (2 mL) and this was added to the GLYMO-MNP material. KOH (50 µL, 1.0 M) was then added to precipitate out the MNPs. The resulting PEG-MNPs were then dispersed in deionised (DI) H_2O at desired concentration. The starting molecular weight of the PEG used was varied to be 400, 1000 and 2070. GLYMO-MNPs were also functionalised with arginine[19] in the same manner whereby arginine (0.005 g) was dissolved in DI H_2O (2 mL) and added to the GLYMO-MNPs in place of PEG.

Citrate-MNPs were synthesised starting with the precipitation of the benzyl alcohol as before. Once all benzyl alcohol was removed from the bare MNPs, sodium citrate in DI H_2O (0.6 g/L) was added to the MNP material to yield a ~1.0 mg/mL MNP dispersion. This dispersion was then placed on a plate shaker at 400 rpm for approx. 4 h. The functionalisation was deemed complete when the dispersion turned from blue-black to a dark brown colour.

Fourier-transform infrared spectroscopy (FTIR) was performed on functionalised MNPs to verify functionalisation (Fig S3). Thermogravimetric analysis (TGA) was also used to confirm functionalisation and also to estimate the number of functional groups per nanoparticle (Fig S4). MNP suspensions were also characterised by dynamic light scattering (DLS) using a Zetasizer Nano ZS (Malvern Instruments, UK). Experiments were performed at 25°C and Z-average hydrodynamic diameter (d_{hyd}) and polydispersity index (PDI) values from cumulants analysis are reported here (Fig S5). A PDI value below 0.2 is indicative of a full particle dispersion. PEG400-, PEG1000- and PEG2070-MNPs, were found to have d_{hyd} (PDI) of 21.5 (0.16), 24.0 (0.16) and 28.0 nm (0.17), respectively. Arginine- and citrate-MNPs were found to have d_{hyd} (PDI) of 28.0 nm (0.16) and 12.0 nm (0.18), respectively. Zeta potential (ζ_p) measurements were performed at 25 °C on the Nano ZS, using the M3-PALS technology for the PEG1000- (-9 mV), citrate- (-27 mV) and arginine- (+30 mV) MNPs (Fig S6).

Agarose gel preparation: To prepare agarose gel (0.3% w/v), 0.06 g of agarose (low EEO content, unless otherwise specified) was weighed out and added to DI water or PBS solute as specified. This mixture was heated and stirred until the agarose had fully dissolved. Once the agarose solution was transparent, glass vials (53 x 16 x 16 mm) were filled with the agarose to a depth of 6 mm and were left to cool at room temperature for 1 h. The vials were then capped and left to solidify overnight at 4°C.

The viscosity of the agarose was measured using a Kinexus Pro+ (Malvern Instruments, UK) rheometer by plate using a shear ramp rate from 10^{-4} to 10^{-1} Hz (n=3).

Measurement of MNP terminal velocity: PEG1000-MNPs at a concentration of ~1.0 mg/mL were prepared. Agarose gels (6 mm depth) were prepared in glass vials, the vials were then placed onto a corner of the neodymium magnet, (Fig S7) where the magnetic force was strongest. Then 100 µL of MNPs (1 mg/mL) was pipetted onto the top surface of the agarose gel to form an even layer of ~1 mm thickness covering the entire upper gel surface (176.6 mm^2), and the vials were capped. The MNPs were observed to migrate towards the base of the vial under the influence of the magnetic field over time. The vials were imaged every 30 min using a standard commercial digital camera. ImageJ software was used to process the images to track the motion of the MNP front in order to calculate MNP experimental terminal velocity (v_{exp}).

Theoretical calculation of MNP terminal velocity: The forces that determine MNP dynamics in viscous media are the drag force (F_D) and the magnetic force (F_M). When these two forces are equal, a constant or terminal particle velocity is achieved. Agarose gels used in this study are biphasic materials comprising hydrated porous polymer networks with the mesh size dependent on the agarose concentration. Hence the appropriateness of applying a continuum model for the forces operating to interpret transport in these circumstances is not certain. Nevertheless, relations have been proposed to describe MNP transport through a viscous medium in an external magnetic field gradient.[14,15]

Based on previous studies[14,15] equation 1 is proposed to calculate the theoretical terminal velocity ,$v_{th,}$ of the MNPs through agarose gels of known viscosity under the influence of an external magnetic field gradient.

$$v_{th} = \frac{\chi_v V_m}{2 r_{hyd}} \cdot \frac{B\nabla B}{\mu_0} \cdot \frac{1}{3\pi\eta\phi} \qquad (1)$$

In this relation the contributions are grouped (from the left) into those relating to the MNPs, to the magnetic force, and to the medium/matrix. χ_v is the volumetric magnetic susceptibility (0.289 here, see Fig S2), V_m is the volume of superparamagnetic material in a single particle (3.69×10^{-25} m^3 determined from core diameter measured using TEM, r_{hyd} is the hydrodynamic radius of the functionalised MNP (m) as measured by DLS; B is the magnetic field strength (specified to be 0.55 T by the distributor), ∇B is the gradient of the magnetic field (45 T m^{-1})[15], μ_0 is the permeability of free space ($4\pi \times 10^{-7}$ T m A^{-1}); ϕ is a scaling factor proposed[18] to account for the tortuous pathway for MNP transport through agarose gels, ϕ increases for highly tortuous paths (one might consider that $1/\phi \rightarrow 0$ for increasingly tortuous paths and $1/\phi \rightarrow 1$ for free diffusion), and η is a viscosity (Pa·s) along that path.

Application of equation 1 assumes that the particles act independently, are spherical, monodisperse, and that the effect of the matrix on MNP transport can be simply parameterised by the product $\eta\phi$ representing the restriction to magnetophoretic transport presented by the biphasic agarose matrix. While these two parameters are difficult to separate, $\eta\phi$ characterises MNP transport through the networks. The % difference (%D) between an experimentally measured, v_{exp}, and theoretical velocity, v_{th} (assuming a value for $\eta\phi$), can be calculated according to equation 2.

$$\%D = \frac{v_{exp} - v_{th}}{v_{th}} \times 100 \qquad (2)$$

Results and discussion

Magnetophoretic mobility of PEG-MNPs in agarose gels

To investigate the behaviour of MNPs in external inhomogeneous magnetic fields through complex media, the magnetophoretic transport of PEG-MNPs through agarose gels was studied. A neodymium alloy magnet was placed under the base of the glass vial containing the agarose and the MNPs (see Methods) to generate the

field gradient. The movement of the MNPs was tracked by video-imaging the MNP front as it moved through the gel. The position of the MNP front was plotted as a function of time (Fig 1). Linear behaviour was observed, demonstrating that a terminal velocity was achieved and maintained for MNPs at the migration front. It can be concluded that the magnetic force exerted was constant over the distance measured and the gel medium was homogenous over the measurable length scale of the optical image (~200 μm). It is also found (Fig 1) that a field gradient is required to initiate and to maintain MNP transport. The motion of the MNPs through the gel is negligible even over many hours in the absence of a gradient. It is also important to note that MNP velocity was not affected by particle concentration in the range 0.5-2.0 mg/mL MNPs (Fig S8), as expected for particles behaving independently.

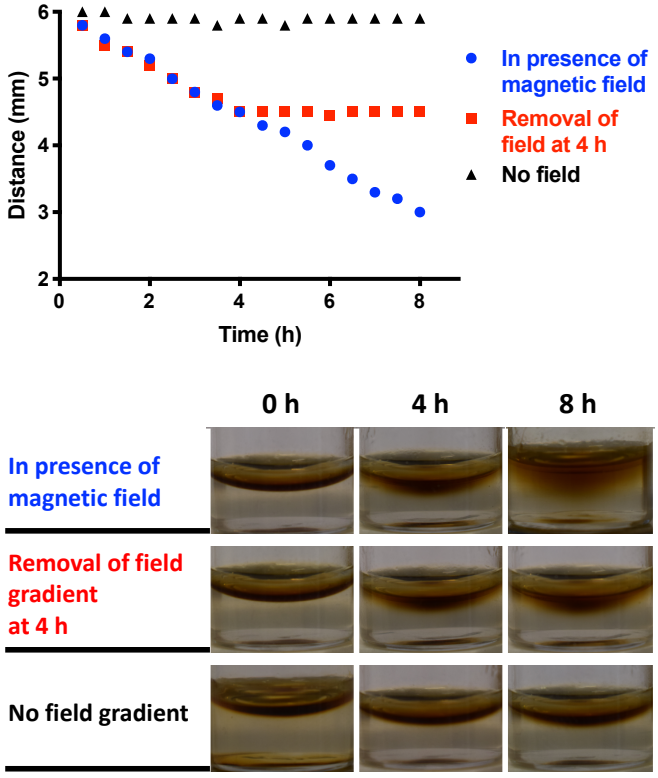

Fig. 1 Top: Transport of ~1.0 mg/mL PEG1000-MNP (d_{hyd} 24.0 nm (0.17)) dispersions in DI H_2O through agarose/DI H_2O (0.3% w/v) as a function of time in the presence of an external magnetic field (n=16); in the absence of an external magnetic field (n=4); and in the presence of an external magnetic for the initial 4 h followed by the removal of field (n=4). Bottom: corresponding digital images showing the MNP front position in the agarose.

In the presence of a constant external magnetic field, v_{exp} was taken as the slope of the linear regression fit on Fig 1C over the linear range of front progression (0.5–8 h). The initial data point (t=0) was omitted as turbulent behaviour was associated with the migration front settling and passing through the upper gel surface. v_{exp} was calculated to be 0.37 ± 0.02 mm/h (n=16) for 24.0 nm (d_{hyd}) PEG1000-MNPs in DI H_2O through agarose (0.3% w/v). The error bars represent the standard deviation on measured velocities for 16 separate gels. Hence the response is highly reproducible for a given MNP batch. Inter-batch variability is also low and is shown in Fig S9. As a linear response was always observed between 6 and *c.*2 mm (R^2>0.99, with no evidence for systematic deviations), for most subsequent experiments data was collected over 4 h. The values for v_{th} (equation 1) calculated using η values of either unloaded gel or pure water and setting ϕ to 1 (unrestricted), differ from the measured v_{exp} values by orders of magnitude. Reasonable agreement was possible for 0.3% w/v agarose using the viscosity of water (η = 0.00089 Pa.s) and ϕ = 0.041. The meaning of ηϕ will be discussed below.

MNPs functionalised with PEG are known to have weak interactions with hydrated polymer matrices due to mostly repulsive steric effects and their near neutral surface charge.[20] To study the effect of the network density on PEG1000-MNP transport, v_{exp} values were measured for different agarose concentrations (Fig 2). In all cases the MNP front moved linearly over the same distance range as before (Fig S10). As the % agarose content was increased, v_{exp} was found to decrease approximately linearly for more dense networks, as expected. Using the extracted v_{exp} values and the measured viscosity (Fig S11) for each gel the tortuosity factor, ϕ, was determined for each sample (Fig 2). It is found that ϕ increases with agarose content (more tortuous paths) as expected.

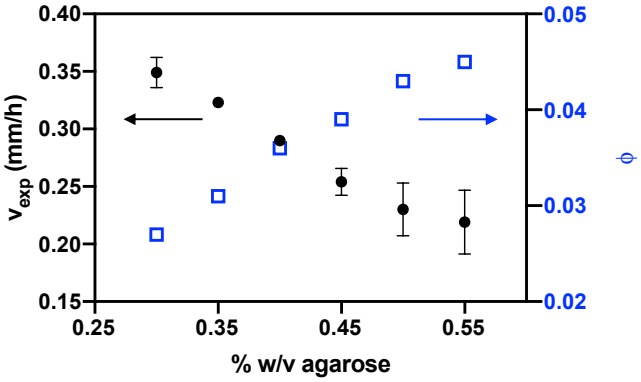

Fig. 2 v_{exp} and corresponding ϕ values obtained for ~1.0 mg/mL PEG1000-MNP dispersions (d_{hyd} 24.0 nm (PDI 0.16)) in DI H_2O, when magnetophoretically transported through agarose gels in DI H_2O (n=4) of varying % w/v.

Interestingly, negligible changes in v_{exp} were observed following repeated magnetophoretic runs through the same gel (Fig S12), which indicates that minimal damage was caused to the networks by MNP transport even at the high MNP concentrations used (~1.0 mg/mL). Over the agarose content range studied, average pore diameters are anticipated to be greater than 300-600 nm[21,22] which is at least an order of magnitude greater than the d_{hyd} values of the MNPs. It is clear that path tortuosity and/or particle graft/network chain entanglement effects are significant for all the gels studied, suggesting that the size of the open pores is not strongly limiting. Previously reported agarose-based ECM biological mimics used agarose content between 0.3 and 0.6% w/v.[2,14] To maintain a high pore volume (to minimise any pore volume effects on transport) and to maintain high v_{exp}, (so that changes in velocity are more easily measured) for the remainder of the current study 0.3% w/v agarose gels were studied.

Turning to the physico-chemical factors relating to the MNPs that influence magnetophoretic mobility; MNPs grafted with PEG of increasing chain length (400, 1000, 2070 Da) were prepared. The d_{hyd} value was observed to increase with increasing chain length (in the range of 21 – 28 nm) and it was found that v_{exp} decreased with chain

length (Table 1). This confirms that hydrodynamic size is a primary factor determining transport; we can infer that the magnetic force is similar in each case as there is a single core per particle. The ϕ value extracted for these three suspensions was found not to vary significantly, as expected, hence a value of 0.041 can be taken as representative of the path through 0.3% w/v agarose (using η of 3080 Pa.s) for suspensions of particles that are not electrostatically stabilised. There may be a small change in the ϕ value extracted on increasing the chain length. This is difficult to confirm given the precision of the experiments. However, it is correlated with a slight increase in ζ_p (Table 1), which suggests the need to fully assess the effect of MNP surface charge on magnetophoretic transport.

TABLE 1 Magnetophoretic parameters for transport of ~1.0 mg/mL PEG-MNPs dispersions in DI H_2O through agarose in DI H_20 (0.3% w/v).

PEG mw (Da)	d_{hyd} (nm)	PDI	ζ_p (mV)	v_{exp} (mm/h)	v_{th} (mm/h)	ϕ
400	21.5	0.17 (±0.01)	-8.6 (±0.07)	0.41 (±0.01)	0.0116	0.042
1000	24.0	0.16 (±0.01)	-9.2 (±0.10)	0.37 (±0.02)	0.0101	0.041
2070	28.0	0.19 (±0.02)	-9.7 (±0.10)	0.32 (±0.01)	0.0086	0.041

Electrostatic effects on magnetophoretic mobility

The effect of ζ_p on MNP magnetophoretic mobility through agarose gels (0.3% w/v) was investigated by varying the surface coating of the MNPs. PEG1000-, arginine- and citrate- functionalised MNPs were prepared, see Methods. The PEG1000-MNP suspensions were anticipated to be sterically stabilised and were found to have a weakly negative ζ_p (-9.0 mV at pH 7.4), arginine-MNPs were found to have a strongly positive ζ_p (+30 mV), while citrate-MNPs had a strongly negative ζ_p (-27 mV). This data is summarised in Table 2. Magnetophoretic transport experiments were performed for the citrate- and arginine-MNPs and it was demonstrated they attained and maintained terminal velocities in a similar manner to PEG1000-MNPs (Fig S13). v_{exp} values were extracted and reported in Table 2. The fact that the velocities were constant suggests that the surface chemistries studied were stable over the full transit through the gels. This was confirmed by re-analysing the recovered MNP suspensions after the transit, and the d_{hyd} and ζ_p values were found to be unchanged (Fig S14).

Table 2 Magnetophoretic parameters for transport of ~1.0 mg/mL PEG1000-, arginine-, and citrate-MNP dispersions in DI H_2O through agarose (0.3% w/v). Colloidal properties of the same dispersions are included.

Surface chemistry	d_{hyd} (nm)	PDI	ζ_p (mV)	v_{exp} (mm/h)	v_{th} (mm/h)	%D
PEG 1000	24.0	0.16 (±0.01)	-9.3 (±0.1)	0.37 (±0.02)	0.37	+0
Arginine	28.0	0.17 (±0.01)	+30 (±1.0)	0.35 (±0.01)	0.32	+8.5
Citrate	12.0	0.18 (±0.02)	-27 (±1.4)	0.63 (±0.02)	0.75	-19.0

For arginine-MNPs ($\zeta_p > 0$), taking the tortuosity, ϕ, to be unchanged, %D (equation 2) was calculated to quantify the difference between the experimentally measured, v_{exp}, and the theoretical velocity, v_{th}. This was determined to be +8.5% in this case, *i.e.* arginine-MNPs move significantly faster than predicted when compared to PEG1000-MNPs ($\zeta_p \leq 0$) of similar d_{hyd}, demonstrating the influence of surface charge. In the case of the citrate-MNPs ($\zeta_p < 0$), %D was negative (-19%). Note that citrate-MNPs had a lower d_{hyd} than PEG1000 or arginine equivalents and v_{exp} was observed to be greater, but by significantly less than is predicted by equation 1. In all cases, as noted above, a single core per particle is assumed and the measured d_{hyd} value used for calculating v_{th}. Hence, we can attribute the negative %D for citrate-MNPs to surface charge as opposed to size effects, an interpretation we confirm below. In summary, significant positive or negative %D values are associated with large positive or negative ζ_p values, respectively, demonstrating the importance of electrostatic interactions between the MNPs and the network chains.

Agarose gels are formed from polysaccharides with the same basic structure but with different substituting groups. The electroendosmosis (EEO) content of the gels is related to the concentration of anionic residues, ester sulphate and pyruvate, present.[23] To further investigate the role of electrostatic interactions between MNPs and the hydrated network during magnetophoresis, three different agarose gel classes were used where the EEO was varied and classed as low, medium and high, see Materials. The magnetophoretic response of three MNP suspensions (PEG1000-, arginine- and citrate-) were tested using each of the three agarose classes. Again, linear transport, the attainment of terminal velocity over the range studied, was observed in all cases. The data is summarised in Fig 3, in this case the velocities are normalised with respect to d_{hyd} of the relevant suspension (v_{exp}/d_{hyd}) to correct for size effects. Note that in all cases d_{hyd} for the recovered suspensions was found to be unchanged after passing through the gels.

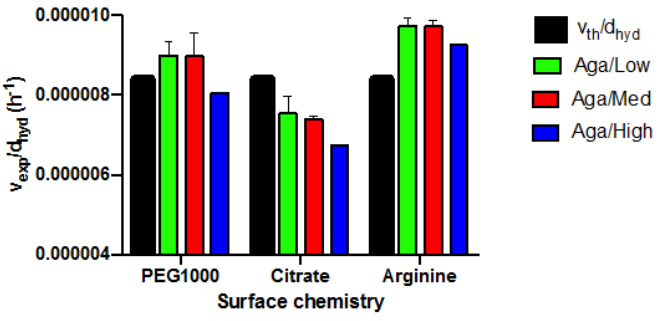

Fig. 3 Normalised magnetophoretic velocities, v_{exp}/d_{hyd}, for PEG1000, citrate-, and arginine-MNP suspensions through the different classes of agarose (Aga/Low, Aga/Med, Aga/High) (0.3% w/v in DI H_2O). Error bars are included for all v_{exp}/d_{hyd} measurements (n=3). The v_{th}/d_{hyd} values are represented as black bars for reference.

The normalised velocities (v_{exp}/d_{hyd}) for each of the functionalised MNPs in Aga/Low, Aga/Med and Aga/High were seen to have similar charge dependence to the suspensions shown in Table 2; arginine-

MNPs moved faster and citrate-MNPs moved slower than PEG1000-MNPs, irrespective of the network charge density. Interestingly, at the highest concentration of fixed anionic charges the normalised velocities of all MNPs decreased, suggestive of an increase in electrostatic interactions between the MNPs and the agarose.

For agarose prepared in DI H_2O, the Debye length, λ_D, of the charges along the network chains is anticipated to be at a maximum. Increasing ionic strength (IS) of the medium will reduce λ_D for the charges on the network chains and the MNP bound ligands and so should influence magnetophoretic transport. Magnetophoretic velocities were measured for transport of PEG1000-, citrate-, arginine-MNPs through Aga/High gels prepared at different IS, again terminal velocities were measured and the results are summarised in Fig 4. Note that the d_{hyd} values of the MNP suspensions were independent of IS across the range studied (Fig S15). It was found that on increasing IS the velocity of the almost neutral PEG1000-MNPs remained unchanged, consistent with minimal electrostatic interactions with the network irrespective of IS. The velocity of negatively charged citrate-MNPs, which was lower than v_{th} in DI H_2O, was found to progressively increase with increasing IS, and the velocity of positively charged arginine-MNPs, higher than v_{th} in DI H_2O, was found to progressively decrease. For both electrostatically stabilised suspensions the normalised velocities approach v_{th} (fixed ϕ of 0.041, corresponding to the path tortuosity observed for PEGylated MNPs) at higher IS, presumably as electrostatic interactions are largely suppressed.

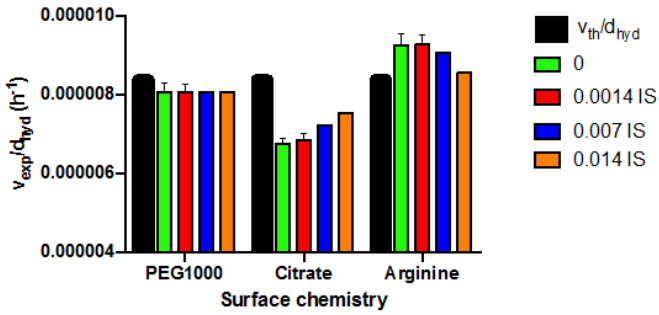

Fig. 4 Normalised magnetophoretic velocities, v_{exp}/d_{hyd}, for PEG1000-, arginine- and citrate-MNP suspensions through agarose (Aga/High, 0.3% w/v). MNP suspensions and agarose gels were prepared in PBS buffer to give IS of 0, 0.0014, 0.007 and 0.014 at pH 7.0. The v_{th}/d_{hyd} values are represented as black bars for reference.

We suggest that during magnetophoresis, negatively charged citrate-MNPs are located predominantly towards the centre of the pores in the agarose gel due to electrostatic repulsion with the pore entrances and walls. The presence of a depleted free void volume close to the pore walls reduces the MNP concentration (and hence flux) and/or reduces the free path, as a result v_{exp} is found to be lower than expected (negative %D, Table 2 and Fig 4). On increasing IS, λ_D is decreased and these electrostatic effects are reduced, increasing v_{exp} for citrate-MNPs (Fig 4). For arginine-MNPs the relative magnetophoretic velocity was greater than expected (positive %D, Table 2 and Fig 4) and decreased with increasing IS (Fig 4). When moving through the network, positively charged arginine-MNPs should undergo attractive interactions with the pore walls. Again, on increasing the IS, these electrostatic effects are reduced, decreasing v_{exp} for arginine-MNPs. Given the large pore sizes it is likely that these effects, which modulate v_{exp} significantly, occur at the pore constrictions (entrances/exits).

The observation that repulsive interactions impede citrate-MNP transport and attractive interactions enhance arginine-MNP transport through the pores is reminiscent of the exclusion enrichment (EE) effect previously described[24,25,26] for molecular motion in charged nanofluidic channels. *Plecis et al.*[24] reported that for channels with dimensions ranging from 2-250 nm, the permeability for small anions and cations undergoing purely electrophoretic transport depends on channel charge as well as the IS of the medium, with reduced mobility for anions which are constrained to the channel centre, and enhanced mobility for the counter-cations[25], largely due to the concentration dependence of the flux. Both effects were found to be suppressed at higher IS.

A similar picture emerges for magnetophoretic transport of charged MNPs though negatively charged agarose pore networks; a schematic representation of pore transport is shown in Scheme 1. We suggest that the electrostatic effect is more pronounced at the pore entrances/exits, where the physical constriction is more comparable to those in nano-channels. Electrostatic effects in soft materials such as polymer gels can be greater than those observed for rigid materials,[27] due to their dynamic nature allowing the charges to be flexible forming mobile electrostatic clouds, and hence would be expected to exert a strong effect at the constrictions. In the scheme the EDLs of the anionic charges of the pore walls form an electrostatic cloud at the entrance of the pore. For negatively charged citrate-MNPs at low IS (A) repulsive electrostatic forces slow particle movement through the pore. At high IS (B), the EDLs on both the charged MNPs and at the pore entrances are decreased, reducing repulsion and increasing flux through the pore under the influence of the magnetic force. Essentially this is due to an increase in the free void volume of the pore. On the other hand for positively charged arginine-MNPs at low IS (C), attractive electrostatic forces between the particles and the fixed negative sites enhance MNP transport through the pore, effectively an 'exclusion enrichment effect'. At high IS (D) reduced EDL overlap weakens this effect reducing MNP velocity.

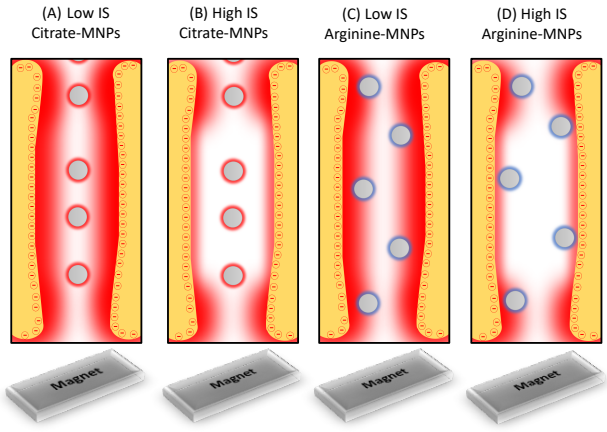

Scheme 1 Schematic representation of transport of citrate- and arginine-MNPs through a pore in agarose gels in low and high IS media.

Finally, the magnetophoretic transport of positively charged arginine-MNPs through Aga/Low and Aga/High gels in both low and

high IS media were measured. The data is summarised in Table 3. The differences in velocity are small in this case, so it is difficult to draw strong conclusions. However, for both EEO types increasing IS reduced v_{exp}, as before, this is again consistent with weaker favourable interactions at the constrictions. However, for both IS values reducing EEO, which should suppress favourable interactions, resulted in an increase in v_{exp}. This suggests the two effects are not strictly additive, but that IS as the more dominant factor for arginine-MNPs, perhaps because higher IS leads to a reduction in λ_D on both the MNPs and the fixed anionic residues. Similar data recorded for citrate-MNP suspensions (Fig S16) supports the suggestion that IS is predominant. In this case for both EEO types increasing IS increased v_{exp}, consistent with weaker unfavourable interactions at the constrictions.

Table 3 Magnetophoretic parameters for transport of ~1 mg/mL arginine-MNP dispersions in aqueous buffered media of varying IS through the different classes of agarose (0.3% w/v) (Aga/Low, Aga/High).

IS	Agarose class (EEO)	v_{exp} (mm/h)	v_{th} (mm/h)	%D
Low (0.0014)	Low	0.35 (0.01)	0.32	+8.5
High (0.014)	Low	0.32 (0.02)	0.32	0
Low (0.0014)	High	0.33 (0.01)	0.32	+3
High (0.014)	High	0.31 (0.01)	0.32	-3

Conclusions

We have presented the first detailed study into magnetophoretic transport of charged and neutral MNPs through hydrogels. The magnetophoretic velocity of MNPs through agarose gels was shown to be independent of their concentration, the d_{hyd} values, always < 30 nm, were found to be unchanged after passing through the gels and the gels were unchanged by the transit. Kuhn et al[15] described experiments performed using larger MNP aggregates (d_{hyd} > 100 nm) for which v_{exp} increased with concentration. As the Fe concentration ranges used were similar to those in the work shown here, we suggest that this effect was most likely due to the particles directly penetrating (and probably damaging) the bulk gel, instead of navigating the porous network as in our case. In any case application of equation 1 is strictly predicated on the MNPs acting independently, the gels being homogeneous and both particles and gels being physically stable, conditions that are strictly met in all the experiments presented here.

Hence it is possible to focus on the response of the gel, which is parameterised by the product $\eta\phi$. We suggest that this product reflects an effective viscosity representing the averaged restriction to MNP motion through a connected tortuous pore path. While the two contributions, η and ϕ, cannot be separated by magnetophoretic measurements, we suggest that the choice of η_{H2O}, suggesting a bulk-like drag force for MNPs within the pores, is useful as it provides a ϕ value that is reflective of the pore connectivity, an approach first suggested by Holligan.[14] This view is supported by the monotonic increase in ϕ with agarose % w/v (Fig 1), by the single ϕ value extracted for 0.3% w/v agarose when only d_{hyd} is varied (Fig 2), and by the collapse of the velocities measured for arginine- and citrate-MNP suspensions back to close to this value when the charge interactions (associated primarily with passage through the pore constrictions) are sufficiently suppressed. From a practical standpoint for PEGylated particles increasing the MNP-graft chain length and reducing the average pore size (by increasing % w/v) in the ranges studied allows v_{exp} to be decreased by *c.* 22 and *c.* 40%, respectively.

For electrostatically stabilised MNPs we have observed, for the first time, a soft hydrogel equivalent of the EE effect that is established for transport of charged molecules through hard nano-pores. Negatively charged MNPs are forced to the centre of the pore constrictions and travel slower than near-neutral MNPs. Positively charged MNPs are attracted by the chains at the constriction and travel faster. These effects can be suppressed by tuning the Debye lengths. Again, from a practical standpoint ionic strength adjustment allows v_{exp} to be reduced by *c.* 8%, for arginine-MNPs and to be increased by *c.* 11%, for citrate-MNPs (for high EEO agarose). Finally, detailed analysis of the interplay of fixed charge content and ionic strength suggest that the latter is the critical factor in determining transport through pore restrictions.

The picture that emerges for MNP transport is a complex interplay of surface charge, pore volume and pore constriction factors combining to effect the magnetophoretic response.[25,26] It is demonstrated that it is possible to significantly modulate terminal velocities during magnetophoretic transport. In ongoing work, we are building on these findings by studying magnetophoretic transport in more complex biological media, such as the extra-cellular matrix, where it is known that electrostatic interactions between particles and the collagenous tissue can be significant.

Conflicts of interest

There are no conflicts to declare.

Acknowledgements

The authors would like to acknowledge Centre for Research in Engineering Surface Technology (CREST) at Technological University Dublin City Campus for the thermogravimetric analysis and the financial support from Science Foundation Ireland under Grant Agreement Nos 13/CDA/2155 and 16/IA/4584.

Notes and references

1 M. Colombo, S. Carregal-Romero, M. F. Casula, L. Gutiérrez, M. P. Morales, I. B. Böhm, J. T. Heverhagen, D. Prosperi and W. J. Parak, *Chem. Soc. Rev.*, 2012, **41**, 4306–4334.

2 J. F. Liu, Z. Lan, C. Ferrari, J. M. Stein, E. Higbee-Dempsey, L. Yan, A. Amirshaghaghi, Z. Cheng, D. Issadore and A. Tsourkas, *ACS Nano*, 2020, **14**, 142–152.

3 E. G. Yarmola, Y. Y. Shah, H. E. Kloefkorn, J. Dobson and K. D. Allen, *Osteoarthritis Cartilage*, 2017, **25**, 1189–1194.
4 E. G. Yarmola, Y. Shah, D. P. Arnold, J. Dobson and K. D. Allen, *Ann. Biomed. Eng.*, 2016, **44**, 1159–1169.
5 D. Chang, M. Lim, J. A. C. M. Goos, R. Qiao, Y. Y. Ng, F. M. Mansfeld, M. Jackson, T. P. Davis and M. Kavallaris, *Front. Pharmacol.*, , DOI:10.3389/fphar.2018.00831.
6 T. Stylianopoulos, M.-Z. Poh, N. Insin, M. G. Bawendi, D. Fukumura, L. L. Munn and R. K. Jain, *Biophys. J.*, 2010, **99**, 1342–1349.
7 N. P. Murphy and K. J. Lampe, *J. Mater. Chem. B*, 2015, **3**, 7867–7880.
8 Z. Tan, D. Dini, F. Rodriguez y Baena and A. E. Forte, *Mater. Des.*, 2018, **160**, 886–894.
9 M. W. Tibbitt and K. S. Anseth, *Biotechnol. Bioeng.*, 2009, **103**, 655–663.
10 J. Lim, C. Lanni, E. R. Evarts, F. Lanni, R. D. Tilton and S. A. Majetich, *ACS Nano*, 2011, **5**, 217–226.
11 P. S. Williams, M. Zborowski and J. J. Chalmers, *Anal. Chem.*, 1999, **71**, 3799–3807.
12 J. Lim, S. P. Yeap, H. X. Che and S. C. Low, *Nanoscale Res. Lett.*, 2013, **8**, 381.
13 B. Shapiro, S. Kulkarni, A. Nacev, S. Muro, P. Y. Stepanov and I. N. Weinberg, *Wiley Interdiscip. Rev. Nanomed. Nanobiotechnol.*, 2015, **7**, 446–457.
14 D. L. Holligan, G. T. Gillies and J. P. Dailey, *Nanotechnology*, 2003, **14**, 661–666.
15 S. J. Kuhn, D. E. Hallahan and T. D. Giorgio, *Ann. Biomed. Eng.*, 2006, **34**, 51–58.
16 A. Tokarev, J. Yatvin, O. Trotsenko, J. Locklin and S. Minko, *Adv. Funct. Mater.*, 2016, **26**, 3761–3782.
17 U. Freudenberg, S. H. Behrens, P. B. Welzel, M. Müller, M. Grimmer, K. Salchert, T. Taeger, K. Schmidt, W. Pompe and C. Werner, *Biophys. J.*, 2007, **92**, 2108–2119.
18 N. Pinna, S. Grancharov, P. Beato, P. Bonville, M. Antonietti and M. Niederberger, *Chem. Mater.*, 2005, **17**, 3044–3049.
19 T. Ninjbadgar and D. F. Brougham, *Adv. Funct. Mater.*, 2011, **21**, 4769–4775.
20 J. S. Suk, Q. Xu, N. Kim, J. Hanes and L. M. Ensign, *Adv. Drug Deliv. Rev.*, 2016, **99**, 28–51.
21 J. Narayanan, J.-Y. Xiong and X.-Y. Liu, *J. Phys. Conf. Ser.*, 2006, **28**, 83.
22 J.-L. Viovy, *Rev. Mod. Phys.*, 2000, **72**, 813–872.
23 N. C. Stellwagen, *Electrophoresis*, 2009, **30 Suppl 1**, S188-195.
24 A. Plecis, R. B. Schoch and P. Renaud, *Nano Lett.*, 2005, **5**, 1147–1155.
25 R. B. Schoch, J. Han and P. Renaud, *Rev. Mod. Phys.*, 2008, **80**, 839–883.
26 G. Bruno, N. Di Trani, R. L. Hood, E. Zabre, C. S. Filgueira, G. Canavese, P. Jain, Z. Smith, D. Demarchi, S. Hosali, A. Pimpinelli, M. Ferrari and A. Grattoni, *Nat. Commun.*, 2018, **9**, 1–10.
27 S. Wu, T. Braschler, R. Anker, F. Wildhaber, A. Bertsch, J. Brugger and P. Renaud, *J. Membr. Sci.*, 2015, **477**, 151–156.